KINETICALLY INDUCED MULTIPLE STEADY STATES DURING ACETYLENE HYDROGENATION

Pavel ČAPEK and Karel KLUSÁČEK

Institute of Chemical Process Fundamentals,
Czechoslovak Academy of Sciences, 165 02 Prague 6-Suchdol

Received October 12, 1989
Accepted December 8, 1989

An isothermal reaction model of acetylene hydrogenation on palladium catalyst is described. Steady-state solutions of the mass balances in a CSTR display regions of multiplicity caused by the very distinct rate and strength of adsorption and desorption of acetylene and hydrogen, respectively. Uniqueness and local stability of this model are investigated numerically; oscillatory behaviour is predicted to be absent for typical conditions.

The interesting phenomena in heterogeneous catalytic systems, multiple steady states and oscillatory behaviour, have attracted considerable interest of chemical engineers in last two decades. Early studies considered these phenomena to result from nonlinearities induced by the coupling of heat generated by the reaction with an Arrhenius temperature dependence of the rate constants or from the interaction of reaction rate and mass transfer. Recent studies have shown that multiplicities and oscillations of system variables may exist even under isothermal conditions and without any mass transport resistances. Kinetically induced isothermal instabilities were studied, for instance, under the assumption that a reaction (CO oxidation on supported Pt) can switch between different mechanisms[1], that an adsorbed species can change[2] between two forms for CO oxidation on Pt, that a catalyst can shift between active and inactive forms[3], that periodic changes can occur in the surface concentrations of a slowly adsorbed nonreacting component[4] and that catalytic activity can vary with surface concentration during reaction of hydrogen and oxygen on nickel[5,6]. Recently, an exponential dependency of the rate constant for surface reaction on the surface coverage has been considered as the cause of instabilities[7-9]. Multiple steady states for stoichiometricly simple heterogeneous catalytic reaction caused by Elovich-type adsorption have been analysed[10]. A comprehensive review[11] on the subject of catalytic multiplicity phenomena has summarized new results.

The purpose of this contribution is to demonstrate that for a catalytic reaction following classic Langmuir–Hinshelwood concept, multiple steady-state regimes can arise as a direct consequence of significantly different strength and rate of adsorption of individual reactants. Whereas most theoretical and experimental studes which

have appeared in the literature focused on the rather simple catalytic reactions (mostly CO oxidation), a more complex acetylene hydrogenation over Pd/Al_2O_3 catalyst has been chosen as an example in this work. Kinetic data (reaction mechanism and rate constants have been taken from the literature[12,14–18]. The discovery of this straightforward model for steady-state multiplicity suggests a useful way of looking at certain multiplicity phenomena in catalysis.

Mathematical Model

The dynamic and steady-state models of acetylene hydrogenation will be derived in this section. The steady-state model will be used for investigation of the possibility of multiple steady-state solutions and their stability. The dynamic model will serve for illustration of the dynamics of surface concentrations when catalytic system is forced to attain a new steady state after step change of feed composition.

Kinetics. It is assumed that acetylene hydrogenation

$$C_2H_2 + H_2 \rightarrow C_2H_4 \qquad (A)$$

$$C_2H_4 + H_2 \rightarrow C_2H_6 \qquad (B)$$

takes place in an isothermal isobaric CSTR without any transport resistance. The mechanism of reactions (*A*) and (*B*) is based on observations published by Bond and co-workers[12] and follows Langmuir–Hinshelwood concept (S denotes active site on the catalyst surface):

$$H_2 + 2\,S \rightleftarrows 2\,H.S \qquad (I)$$

$$C_2H_2 + 2\,S \rightleftarrows C_2H_2.S_2 \qquad (II)$$

$$C_2H_2.S_2 + H.S \rightleftarrows C_2H_3.S_2 + S \qquad (III)$$

$$C_2H_3.S_2 + H.S \rightarrow C_2H_4.S + 2\,S \qquad (IV)$$

$$C_2H_4 + S \rightleftarrows C_2H_4.S \qquad (V)$$

$$C_2H_4.S + H.S \rightleftarrows C_2H_5.S + S \qquad (VI)$$

$$C_2H_5.S + H.S \rightarrow C_2H_6 + 2\,S\,. \qquad (VII)$$

Hydrogen can be weakly adsorbed also in molecular form. This step is assumed to

be very slow[12] in comparison with dissociative step (*I*) and is neglected in this work to reduce the model complexity.

For easy manipulation, reaction components are denoted as:

$C_2H_2 \equiv 1$, $C_2H_4 \equiv 2$, $C_2H_6 \equiv 3$, $H_2 \equiv 4$, inert $\equiv 5$, $H.S \equiv 6$, $C_2H_2.S_2 \equiv 7$, $C_2H_3.S_2 \equiv 8$, $C_2H_4.S \equiv 9$, $C_2H_5.S \equiv 10$, $S \equiv 11$.

Dynamic model. The dynamic mass balances in an isothermal isobaric CSTR give for gaseous components

$$f_i \equiv (\mathrm{d}y_i/\mathrm{d}t) = \sigma^0 y_i^0 - \sigma y_i + \phi R_i\,, \quad i = 1, \ldots, 5 \tag{1}$$

and for surface species

$$f_i \equiv (\mathrm{d}y_i/\mathrm{d}t) = R_i\,, \quad i = 6, \ldots, 11\,. \tag{2}$$

In Eqs (*1*) and (*2*) y_i are mole fractions of i-th gaseous component ($i = 1, \ldots, 5$) or dimensionless concentrations of i-th surface species ($i = 6, \ldots, 11$) (for definition of these and other dimensionless variables see Symbols).

Eleven dynamic balance equations (*1*) and (*2*) may be reduced to nine because in an isobaric CSTR $\sum y_i = \sum y_i^0 = 1$ ($i = 1, \ldots, 5$) and under the assumption of a constant total concentration of active sites $\sum y_i = 1$ ($i = 6, \ldots, 11$). Under these circumstances only nine equations of system (*1*) and (*2*) are independent. From practical reasons the balance equations for inert ($i = 5$) and free active centres ($i = 11$) were omitted.

The outlet space velocity, σ, generally differs from its inlet value, σ^0. This is caused by the reaction stoichiometry and (under unsteady conditions) by the dynamics of adsorption/desorption steps. In an isobaric CSTR the following relation can be derived[13].

$$\sigma = \sigma^0 + \phi \sum_{i=1}^{4} R_i\,. \tag{3}$$

Assuming the validity of mass action law for the (pseudo) elementary steps (*I*)–(*VII*), the rates of individual steps (*I*)–(*VII*) are expressed as

$$r_I = k_I y_4 y_{11}^2 - k_I' y_6^2 \tag{4a}$$

$$r_{II} = k_{II} y_1 y_{11}^2 - k_{II}' y_7 \tag{4b}$$

$$r_{III} = k_{III} y_6 y_7 - k_{III}' y_8 y_{11} \tag{4c}$$

$$r_{IV} = k_{IV} y_6 y_8 \tag{4d}$$

$$r_V = k_V y_2 y_{11} - k_V' y_9 \tag{4e}$$

$$r_{VI} = k_{VI} y_6 y_9 - k'_{VI} y_{10} y_{11} \tag{4f}$$

$$r_{VII} = k_{VII} y_6 y_{10} \,. \tag{4g}$$

Numerical values of forward (k_i) and reverse (k'_i) rate constants based on available literary data on acetylene hydrogenation[12,14–18] are summarized in Table I.

For rates of formation of individual reaction components it holds

$$R_i = \sum_{k=I}^{VII} a_{ik} r_k \,, \quad i = 1, \ldots, 10; \; i \neq 5 \,, \tag{5}$$

where a_{ik} is the stoichiometric coefficient of i-th component in k-th elementary step of the mechanism (*I*)–(*VII*), i.e.:

$$\begin{aligned} R_1 &= -r_{II}; \; R_2 = -r_V; \; R_3 = r_{VII}; \; R_4 = -r_I \,; \\ R_6 &= 2r_I - r_{III} - r_{IV} - r_{VI} - r_{VII}; \; R_7 = r_{II} - r_{III} \,; \\ R_8 &= r_{III} - r_{IV}; \; R_9 = r_{IV} + r_V - r_{VI}; \; R_{10} = r_{VI} - r_{VII} \,. \end{aligned} \tag{6}$$

Steady-state model. The steady-state solution of the system (*1*) and (*2*) satisfies the set of nonlinear algebraic equations

$$f_i = 0 \,, \quad i = 1, \ldots, 10 \,; \; i \neq 5 \tag{7}$$

and the steady-state version of Eq. (*3*) holds:

$$\sigma = \sigma^0 + \phi R_4 \,. \tag{8}$$

TABLE I
Rate constants of reaction sequence (*4*)

Step i	k_i, s^{-1}	k'_i, s^{-1}
(*I*)	146·5	75·0
(*II*)	48·85	0·01
(*III*)	0·25	0·0125
(*IV*)	1·5	0·0
(*V*)	0·896	0·056
(*VI*)	2·5	0·005
(*VII*)	40·0	0·0

The steady-state model (Eqs (6)–(8)) could be reduced by substituting for individual concentrations using stoichiometric relations. However, the resulting rather complicated algebraic equations are difficult to handle. Thus, similarly as for the dynamic case, nine equations were solved:

$$\sigma^0 y_i^0 - \sigma y_i + \phi R_i = 0\,, \quad i = 1, \ldots, 4 \tag{9a}$$

$$R_i = 0\,, \quad i = 6, \ldots, 10 \tag{9b}$$

with σ given by Eq. (8) and R_i from Eq. (6).

For illustrative purposes it is useful to define the conversions of acetylene, x_1, and hydrogen, x_4 as follows:

$$x_1 = 1 - (\sigma y_1/(\sigma^0 y_1^0))\,; \quad x_4 = 1 - (\sigma y_4/(\sigma^0 y_4^0)) \tag{10}$$

and the differential reaction selectivity as follows:

$$S_D = R_2/(R_2 + R_3)\,. \tag{11}$$

Uniqueness and Stability of the Steady-State Solution

Steady-state model (set of Eqs (9)) contains nine state variables (mole fractions and surface concentrations) y_i ($i = 1, \ldots, 10$; $i \neq 5$) and eighteen parameters: twelve rate constants (k_i, k_i', see Eqs (4)), four inlet mole fractions of gaseous components y_i^0 ($i = 1, \ldots, 4$), capacity factor ϕ and inlet space velocity σ^0. Most of these parameters are fixed by the reactor configuration and/or experimental conditions, others are given by the reaction kinetics. In the following numerical example it will be shown that under practical circumstances the number of variable parameters can be easily reduced to just one.

The function relating the vector of state variables y_i to the arbitrary chosen parameter may be viewed as branches beginning at specific branch points. In our analysis, we shall deal with bifurcation points, i.e. with points where branching of the steady-state solution of the system (9) occurs. The necessary condition for a bifurcation point is given[19] by the singularity of the Jacobi matrix, $\boldsymbol{J}$, of Eqs (9)

$$\det \boldsymbol{J} = 0 \tag{12}$$

with elements

$$g_{ij} = (\partial f_i/\partial y_j)\,, \quad i, j = 1, \ldots, 10;\ i, j \neq 5\,. \tag{13}$$

The branch points of the steady-state solution can be determined also from eigen-

values of $\boldsymbol{J}$, because at a point of real bifurcation, zero becomes an eigenvalue of $\boldsymbol{J}$. At this point, the zero eigenvalues crosses the imaginary axis in the complex plane and a new branch of the stationary solution arises. Complex bifurcation point appears when a pair of complex-conjugate eigenvalues crosses the imaginary axis and a branch of periodic solutions (limit cycles) may arise (see Kubíček and Marek[19] for details).

Eqs (*9*) and condition (*12*) form a set of ten nonlinear algebraic equations for ten coordinates of the real bifurcation point (y_i^*, $i = 1, \ldots, 10$; $i \neq 5$ and one chosen variable parameter).

Numerical analysis of the local stability of steady-state solution requires an investigation of eigenvalues of the Jacobian $\boldsymbol{J}$ evaluated for the stationary solution in question[20]. If the real part of every eigenvalue λ_i is negative, i.e.

$$\operatorname{Re} \lambda_i < 0\,, \quad i = 1, \ldots, 9\,, \tag{14}$$

the steady-state solution is locally stable for that particular value of chosen variable parameter, i.e. system returns to the original steady state after small perturbations.

Numerical Example

As has been mentioned above the number of variable parameters of system (*9*) can be reduced. In our case, ϕ is assumed to be invariant (it is given by the catalyst properties, reaction conditions and the reactor geometry) and rate constants k_i, k_i' (Eqs (*4*)) are fixed in the isothermal case. Furthermore, if the reactor feed does not contain ethylene and ethane ($y_2^\circ = y_3^\circ = 0$) and the sum of inlet mole fractions of acetylene and hydrogen, y_1° and y_4°, is kept constant ($y_1^\circ + y_4^\circ = \text{const.}$), then for fixed inlet space velocity, σ°, an effect of only one system parameter, y_1°, needs to be examined.

To demonstrate the method of the numerical analysis of uniqueness and stability of steady-state solution of acetylene hydrogenation, the following values are considered

$$\phi = 0{\cdot}325\,, \quad y_1^\circ + y_4^\circ = 0{\cdot}2\,,$$
$$y_2^\circ = y_3^\circ = 0\,, \quad y_5^\circ = 0{\cdot}8\,. \tag{15}$$

The employed constants k_i and k_i' are summarized in Table I; the calculations were carried out for six different inlet space velocities σ°: 0·005; 0·01; 0·0175; 0·025; 0·05 and 0·1 s^{-1}.

To determine the coordinates of real bifurcation points, the system of nonlinear algebraic equations (*9*) and (*12*) was solved numerically by a standard routine ZSCNT (ref.[21]). The obtained results are summarized in Table II.

As it's apparent from Table II, the width of the hysteresis loop depends on the space velocity used. For low space velocities there are no bifurcations of steady-state solutions and for the space velocity $\sigma^0 = 0{\cdot}05\ s^{-1}$ the width of hysteresis loop reaches a maximum value. The results obtained for this space velocity after the evaluation of the conversions of acetylene, x_1, and hydrogen, x_4, are plotted in Fig. 1, the bifurcations of the selectivity, S_D, are shown in Fig. 2.

TABLE II
Bifurcation points of steady-state solution for different space velocity σ^0

σ^0, s^{-1}	Bifurcation point I y_1^{0*}	Bifurcation point II y_1^{0*}
0·005	no bifurcation	no bifurcation
0·010	no bifurcation	no bifurcation
0·0175	0·0641	0·0621
0·025	0·0603	0·0553
0·050	0·0462	0·0408
0·100	0·0292	0·0280

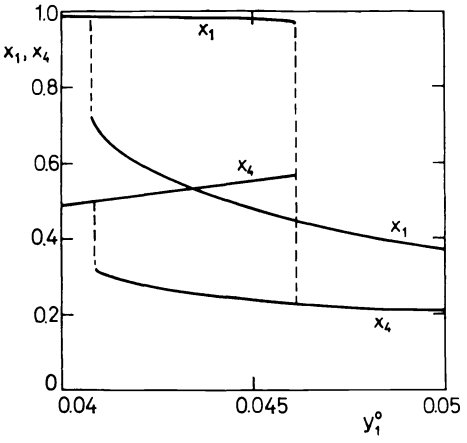

FIG. 1
Multiple steady states in a CSTR. Conversion of acetylene, x_1, and hydrogen, x_4, as a function of feed composition for space velocity $\sigma^0 = 0{\cdot}05\ s^{-1}$

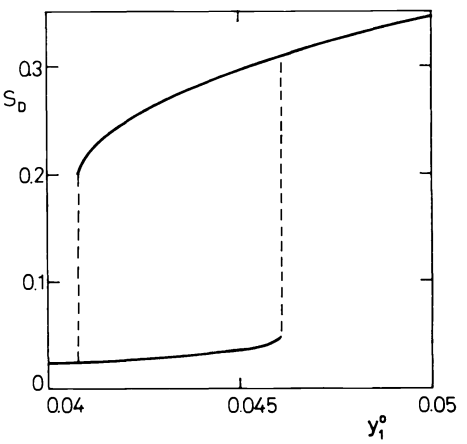

FIG. 2
Multiple steady states in a CSTR. Differential selectivity, S_D, as a function of feed composition for space velocity $\sigma^0 = 0{\cdot}05\ s^{-1}$

The multiplicity of steady states is also indicated in Fig. 3 where the value of det $\boldsymbol{J}$ is shown as a function of the feed composition for the upper branch of steady-state solutions from Fig. 1. When y_1^0 corresponds to the bifurcation point for space velocity $\sigma^0 = 0{\cdot}05\ s^{-1}$ (see Table II), det $\boldsymbol{J}$ becomes zero in accordance with Eq. (*12*).

A physical explanation of multiplicities follows from the conditions on the catalyst surface, as shown in Figs 4a, b. The solution of steady-state equations (*9*) leads to a multiplicity of surface concentratios of hydrogen, y_6, and acetylene, y_7, between both bifurcation points.

A multiplicity of surface concentrations is caused by the magnitude of individual rate constants given in Table I. Dissociative adsorption of hydrogen (step (*I*)) is very fast, however, due to the high desorption rate of adsorbed hydrogen, the resulting adsorption equilibrium constant of hydrogen $K_4 = k_I/k_I' = 1{\cdot}953$ is very low (adsorption of hydrogen is fast and weak) in comparison with that for acetylene $K_1 = k_{II}/k_{II}' = 4\,885$ (adsorption of acetylene is slow and strong). Under these circumstances it depends on the history of the catalytic system, i.e. on the initial conditions, which final steady state is reached in the region of multiplicities. If the system starts from the free (uncovered) surface or from the surface covered by hydrogen then due to the very high adsorption rate of hydrogen the final surface concentrations of hydrogen and acetylene are high enough to maintain the system on the upper branch of conversions (Fig. 1). On the other hand if the system starts from the surface covered by very strongly adsorbed acetylene then surface concentration of hydrogen is not able to reach sufficiently high value necessary for the upper branch and the final steady state is on the lower branch in Fig. 1. The dynamic behaviour of the catalytic surface is apparent from Fig. 5. The trajectories of surface concentra-

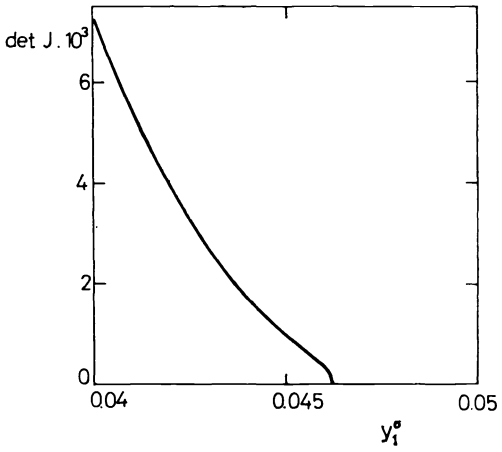

FIG. 3

Determinant of Jacobi matrix of the stationary system for different feed compositions for the upper branch of steady-state solutions in Fig. 1

tions in the phase plane $y_6 - y_7$ were obtained from the numerical integration of dynamic system balances (*1*) and (*2*) using Gear's algorithm[22]. To generate the curves in Fig. 5, the system was started at a steady state (different for different curves) and then the feed composition was abruptly changed to the composition $y_1^0/y_4^0/y_5^0 = 0{\cdot}044/0{\cdot}156/0{\cdot}8$ which is in the multiplicity region (cf. Figs 1 and 2). In Fig. 5, trajectory 1 arises from initial surface concentrations $y_6 = 0{\cdot}385$ and $y_7 = 0$ corresponding to the steady state for feed composition $y_1^0/y_4^0/y_5^0 = 0/0{\cdot}2/0{\cdot}8$ and this trajectory reaches a new steady state at point P_1. At this point ($y_6 = 0{\cdot}173$, $y_7 =$

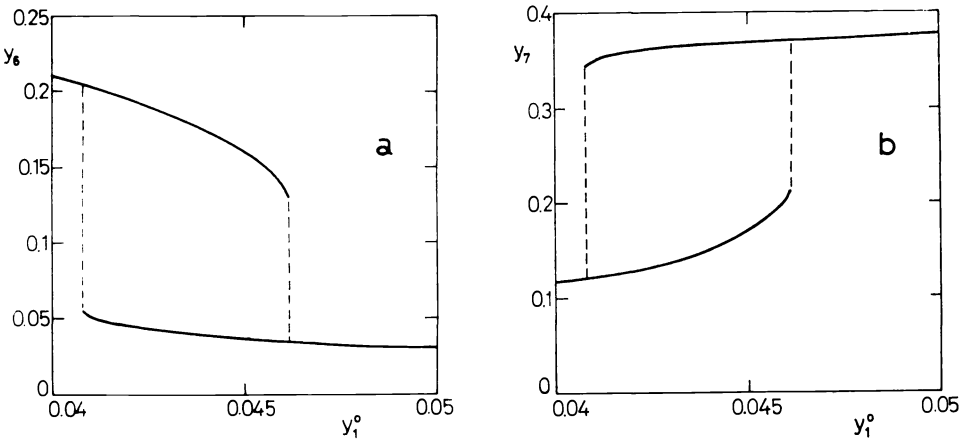

FIG. 4

Multiplicity of steady-state surface concentrations of a hydrogen, y_6, and b acetylene, y_7, for steady states in Figs 1 and 2

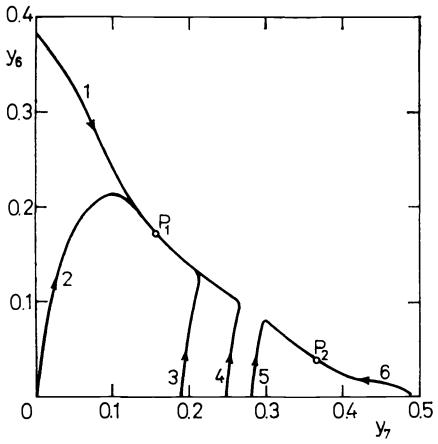

FIG. 5

Phase plane of surface concentrations with two possible steady states for feed composition $y_1^0/y_4^0/y_5^0 = 0{\cdot}044/0{\cdot}156/0{\cdot}8$ in the region of multiplicities for space velocity $\sigma^0 = 0{\cdot}05\ s^{-1}$. Initial conditions for individual trajectories are given in the text

= 0·157) conversions $x_1 = 0{\cdot}983$, $x_4 = 0{\cdot}545$ correspond to the upper-branch of steady-state solutions (cf. Fig. 1) for the feed composition and space velocity used. Point P_1 is also attained if the surface of catalyst is initially clean ($y_6 = y_7 = 0$, trajectory 2) or if the system starts from initial surface concentrations $y_6 = 0$ and $y_7 = 0{\cdot}189$ corresponding to the steady state for feed composition $y_1^0/y_4^0/y_5^0 =$ = 0·0001/0/0·9999 (trajectory 3) or if the initial surface concentrations are $y_6 = 0$ and $y_7 = 0{\cdot}248$, i.e. the steady state for feed composition $y_1^0/y_4^0/y_5^0 = 0{\cdot}0002/0/$ /0·9998 (trajectory 4). On the other hand, trajectory 5 arises from the combination of surface concentrations $y_6 = 0$ and $y_7 = 0{\cdot}281$ corresponding to the steady state feed composition $y_1^0/y_4^0/y_5^0 = 0{\cdot}0003/0/0{\cdot}9997$ and trajectory 6 begins at surface concentrations $y_6 = 0$ and $y_7 = 0{\cdot}489$, i.e. at steady state for feed composition $y_1^0/y_4^0/y_5^0 = 0{\cdot}2/0/0{\cdot}8$ and it attains point P_2, where the conversions $x_1 = 0{\cdot}512$, $x_4 = 0{\cdot}248$ correspond to the lower branch of the steady-state plot (Fig. 1). The trajectories approach the final steady state without any oscillatory behaviour.

The illustrative example of the effect of individual rate constants on the dynamic behaviour of the catalyst surface is shown in Figs 6a, b. The curves were obtained by numerical integration[22] of dynamic balances (*1*) and (*2*). The integration started from the clean catalyst ($y_i = 0$, $i = 6, \ldots, 9$) and in time $t = 0$ the feed composition was changed in the step manner from pure inert ($y_5^0 = 1$) to $y_1^0/y_4^0/y_5^0 = 0{\cdot}04/0{\cdot}16/0{\cdot}8$ (Fig. 6a) and to $y_1^0/y_4^0/y_5^0 = 0{\cdot}05/0{\cdot}15/0{\cdot}8$ (Fig. 6b). In Fig. 6a, where the feed composition corresponds to the upper branch of the steady-state conversions (cf. Fig. 1),

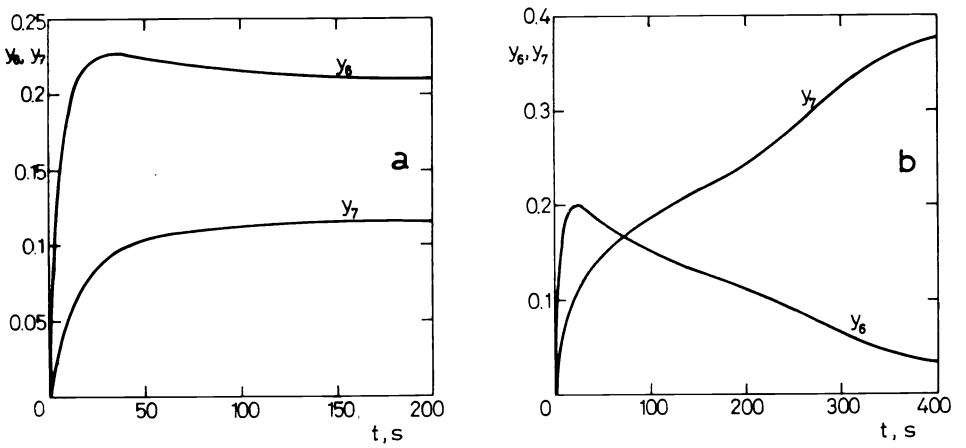

FIG. 6

Transients of surface concentrations of hydrogen, y_6, and acetylene, y_7, after step change of the feed composition: a pure inert $\rightarrow y_1^0/y_4^0/y_5^0 = 0{\cdot}04/0{\cdot}16/0{\cdot}8$ and b pure inert $\rightarrow y_1^0/y_4^0/y_5^0 =$ = 0·05/0·15/0·8

the adsorbed acetylene (y_7) is continuously consumed by the surface reactions. Its surface concentration, y_7, is kept rather low due to the low concentration of acetylene in the gaseous phase and also because the rate constant for acetylene adsorption (k_{II}) is small when compared with adsorption rate constant for hydrogen (k_I). The system attains a new steady state in about 200 s and concentrations of both hydrogen and acetylene are high enough to maintain conversions x_1, x_4 on the upper branch. On the other hand if the feed composition changes in time $t = 0$ to that having higher acetylene concentration than corresponds to the upper bifurcation point (Fig. 5b), the high concentration of acetylene in gaseous phase of a CSTR ensures sufficiently fast adsorption of acetylene and its adsorbed form gradually replaces adsorbed hydrogen on the catalyst surface during the transient of the catalytic system to a new steady state. The concentration of adsorbed acetylene (y_7) is not significantly lowered by desorption because the desorption constant of acetylene (k'_{II}) is very low. The high surface concentration of acetylene combined

TABLE III
Eigenvalues of Jacobi matrix (model parameters as in Fig. 1)

Feed composition $y_1^0/y_4^0/y_5^0$	Eigenvalues λ_i ($i = 1, \ldots, 9$)
0·03/0·17/0·80	$(-4{\cdot}706 \cdot 10^{-2})$; $(-1{\cdot}801 \cdot 10^{-1})$ $(-1{,}334 \cdot 10^{2})$; $(-2{\cdot}958 \cdot 10^{-2})$ $(-1{\cdot}080 \cdot 10^{1})$; $(-7{\cdot}740 \cdot 10^{-2})$ $(-5{\cdot}116)$; $(-4{\cdot}152 \cdot 10^{-1})$ $(-7{\cdot}815 \cdot 10^{-1})$
0·045/0·155/0·80 (upper branch)	$(-4{\cdot}567 \cdot 10^{-2})$; $(-1{\cdot}239 \cdot 10^{-2})$ $(-7{\cdot}447 \cdot 10^{1})$; $(-8{\cdot}894 \cdot 10^{-2} + 2{\cdot}325 \cdot 10^{-2}\,\mathrm{i})$ $(-6{\cdot}400)$; $(-8{\cdot}894 \cdot 10^{-2} - 2{\cdot}325 \cdot 10^{-2}\,\mathrm{i})$ $(-2{\cdot}919)$; $(-2{\cdot}498 \cdot 10^{-1})$ $(-5{\cdot}783 \cdot 10^{-1})$
0·045/0, 155/0·80 (lower branch)	$(-4{\cdot}816 \cdot 10^{-2})$; $(-3{\cdot}175 \cdot 10^{-2})$ $(-1{\cdot}735 \cdot 10^{1})$; $(-4{\cdot}503 \cdot 10^{-2} + 6{\cdot}381 \cdot 10^{-3}\,\mathrm{i})$ $(-1{\cdot}445)$; $(-4{\cdot}503 \cdot 10^{-2} - 6{\cdot}381 \cdot 10^{-3}\,\mathrm{i})$ $(-5{\cdot}787 \cdot 10^{-1})$; $(-6{\cdot}053 \cdot 10^{-2})$ $(-1{\cdot}520 \cdot 10^{-1})$
0·05/0·15/0·80	$(-4{\cdot}847 \cdot 10^{-2})$; $(-4{\cdot}003 \cdot 10^{-2} + 6{\cdot}507\,\mathrm{i})$ $(-1{\cdot}464 \cdot 10^{1})$; $(-4{\cdot}003 \cdot 10^{-2} - 6{\cdot}507\,\mathrm{i})$ $(-1{\cdot}204 .)$; $(-4{\cdot}402 \cdot 10^{-2})$ $(-5{\cdot}802 \cdot 10^{-1})$; $(-5{\cdot}311 \cdot 10^{-2})$ $(-1{\cdot}287 \cdot 10^{-1})$

with the low concentration of adsorbed hydrogen results in the drop to the lower branch of the steady-state solutions.

The stability of the steady-state solutions for parameters (*15*) has been examined by investigation of eigenvalues of the Jacobian, **J**, for a different discrete inlet stream compositions. The examples of results obtained for space velocity $\sigma^0 = 0{\cdot}05\ s^{-1}$ by the use of a standard routine EIGRF (ref.[21]) are shown in Table III. As can be seen, the necessary condition for system stability (i.e. negative real parts of eigenvalues; Eq. (*14*)) is satisfied within the whole interval of inlet stream compositions considered (except at both bifurcation points where the system has zero eigenvalues). In the region of multiple steady states, two different sets of eigenvalues for one reactor feed composition may be obtained but both sets satisfy stability conditions (*14*). Similar results were obtained also for other space velocities. The above numerical analysis shows that there are no dynamic instabilities that give rise to periodic oscillations system variables for the parameters given by Eq. (*15*) and Table I.

CONCLUSION

It has been shown that for the acetylene hydrogenation a region of multiple steady state exists. Within this region, the steady state depends on the system history. The reaction mechanism and values of kinetic constants have been taken from literature. To locate the real bifurcation points, a numerical technique was used that provided a simple analysis of a system with many variables. The multiplicity of steady states arises as a consequence of a large differences between adsorption and desorption rate constants of reaction components when relatively weakly adsorbed hydrogen adsorbs very quickly in comparison with strongly adsorbed acetylene.

SYMBOLS

a_{ik}	stoichiometric coefficient of i-th component in k-th elementary step
c_i	molar concentration of i-th gaseous component ($i = 1, \ldots, 5$) or i-th surface species ($i = 6, \ldots, 11$)
c_L	total molar concentration of active sites (in this work, $0{\cdot}05\ mol\ kg^{-1}$)
c_T	total molar concentration in gas phase (in this work, $38{\cdot}43\ mol\ m^{-3}$)
f_i	function given by mass balance equations
g_{ij}	element of Jacobian **J**
J	Jacobian
k_i, k'_i	rate constants (see Table I)
r_k	rate of k-th step
R_i	rate of formation of i-th component
S_D	differential selectivity (Eq. (*11*))
t	time
V	reactor free volume (in this work, $2{\cdot}0 \cdot 10^{-5}\ m^3$)
W	catalyst weight (in this work, $5{\cdot}0 \cdot 10^{-3}\ kg$)

x_i conversion of acetylene ($i = 1$) and hydrogen ($i = 4$), Eq. (*10*)
y_i $= c_i/c_T$, mole fraction of gaseous component ($i = 1, \ldots, 5$) or ($= c_i/c_L$) dimensionless surface concentration ($i = 6, \ldots, 11$)
ϕ $= Wc_L/(Vc_T)$, capacity factor
λ_i eigenvalue of Jacobi matrix
σ space velocity

Subscripts

1, ..., 5 for gas components C_2H_2, C_2H_4, C_2H_6, H_2, inert
6, ..., 11 for surface components H.S, $C_2H_2.S_2$, $C_2H_3.S_2$, $C_2H_4.S$, $C_2H_5.S$, S

Superscripts

° reactor input
* bifurcation point

REFERENCES

1. McCarthy E., Zahradník J., Kucsynski G. C., Carberry J. J.: J. Catal. *39*, 29, (1975).
2. Hugo P., Jakubith M.: Chem. Ing. Techn. *44*, 383 (1972).
3. Beusch H., Feiguth P., Wicke E.: Chem.-Ing.-Tech. *44*, 445 (1972).
4. Eigenberger G.: Chem. Eng. Sci. *33*, 1255 (1978).
5. Belyaev V. D., Slinko M. M., Timoshenko V. I., Slinko M. G.: Kinet. Katal. *14*, 810 (1973).
6. Belyaev V. D., Slinko M. G., Timoshenko V. I.: Kinet. Katal. *16*, 555 (1975).
7. Pikios C. A., Luss D.: Chem. Eng. Sci. *32*, 191 (1977).
8. Ivanov E. A., Chumakov G. A., Slinko M. G., Bruns D. D., Luss D. D.: Chem. Eng. Sci. *35*, 795 (1980).
9. Jayaraman V. K., Ravi Kumar V., Kulkarni B. D.: Chem. Eng. Sci. *36*, 1731 (1981).
10. Klusáček K., Hudgins R. R., Silveston P. L.: Chem. Eng. Sci. *44*, 2377 (1989).
11. Razon L. F., Schmitz R. A.: Chem. Eng. Sci. *42*, 1005 (1987).
12. Bond G. C., Wells P. B.: J. Catal. *5*, 65 (1966).
13. Klusáček K.: Collect. Czech. Chem. Commun. *49*, 170 (1984).
14. Webb G. in: *Comprehensive Chemical Kinetics*, Vol. 20, *Heterogeneous Catalytic Reactions* (C. H. Bamford and C. F. H. Tipper, Eds), p. 50. Elsevier, Amsterdam 1978.
15. Bond G. C., Wells P. B.: J. Catal. *5*, 419 (1966).
16. Tamaru K.: Bull. Chem. Soc. Jpn. *23*, 64 (1950).
17. Bond G. C., Dowen D. A., Mackenzie N.: Trans. Faraday Soc. *54*, 1537 (1958).
18. Inoue Y., Yasumori I.: J. Phys. Chem. *75*, 880 (1971).
19. Kubíček M., Marek M.: *Computational Methods in Bifurcation Theory and Dissipative Structures*. Springer, New York 1983.
20. Cesari L.: *Asymptotic Behavior and Stability Problems in Ordinary Differential Equations*. Springer, New York 1971.
21. *Library of Standard Fortran Routines*, IMSL, Release 1980. IMSL Inc., Houston, Texas, U.S.A. 1980.
22. Hindmarsh A. C.: *GEAR: Ordinary Differential Equation System Solver*. Lawrence Livermore Laboratory, Report UCID-30001, Revision 3 (1974).

Translated by the author (K.K.).